Eur. Phys. J. Appl. Phys. **45**, 21202 (2009)
DOI: 10.1051/epjap/2009001

THE EUROPEAN PHYSICAL JOURNAL APPLIED PHYSICS

A study of the ultra-cold neutron up-scattering at reflection from solid surface

Y.N. Pokotilovski[1,a], M.I. Novopoltsev[2], and P. Geltenbort[3]

[1] Joint Institute for Nuclear Research, 141980 Dubna, Moscow region, Russia
[2] Mordovian State University, 430000 Saransk, Russia
[3] Institut Laue-Langevin, BP 156, 38042 Grenoble Cedex 9, France

Received: 25 October 2007 / Received in final form: 15 January 2008 / Accepted: 23 November 2008
Published online: 31 January 2009 –

Abstract. We describe a method and present the results of the measurements of spectral change of stored ultra-cold neutrons and the sub-barrier neutron up-scattering from solid surfaces to the energy range higher than the boundary energy of the sample. The method consists in measuring the neutron absorption curves as a function of UCN storage time and the thickness of the absorbers. The quasi-elastic and inelastic UCN up-scattering probability is determined at room temperature. The neutron spectra are inferred in monochromatic and more detailed approximations.

PACS. 28.20.Cz Neutron scattering – 29.30.Hs Neutron spectroscopy – 61.12.-q Neutron diffraction and scattering

1 Introduction

Ultra-cold neutrons [1] (UCN, the energy below ∼0.2–0.3 μeV) confined in traps are used for studying the fundamental properties of the neutron [2,3].

However, the measured values of the neutron loss probability per one collision with the trap wall are still inconsistent with the calculated ones from the measured cold neutron transmission cross sections or on the basis of reasonable dynamic models [4]. The cause of anomalous UCN losses is still understood incompletely.

Progress in understanding the interactions of UCN with surface is important as an additional technique for surface studies and for particle physics.

A number of recent experiments have shown that there are small (∼10^{-7} eV) UCN energy transfers at the UCN reflection from the walls of storage volumes [4–12]. The reported probability of this effect per reflection was from ∼10^{-5} in the first publications for metal surfaces and for the surface of liquid fluorinated oil (Fomblin), to ∼10^{-7} in the most recent publications. The UCN down-scattering with lower probability has been reported in reference [12,13].

The low-energy up-scattering from liquid surface was described as quasi-elastic neutron scattering by viscoelastic surface waves [14–16]. As for the solid reflecting surface the nature of the effect is not quite clear. The probability of phonon up-scattering with very small neutron energy changes should be many orders of magnitude lower.

Two mechanisms were proposed to explain this extraordinary large scattering probability to small neutron momentum space volume: diffusive motion of absorbed and dissolved hydrogen [17], and the motion of nanoparticles at the surface [18,19]. But in more recent experiments [20] it was found that the probability of "small heating" at UCN reflection from solid walls is ∼10^{-8} or lower, the probability of the effect at the reflection from viscous liquid fluorinated oil being of order of 10^{-5} – in good agreement with the previous observations [4–10] and calculations of [14]. The experimental setups and the methods of measurements in [4–10] and [20] were close, the main contradiction concerned the efficiency of detection of up-scattered neutrons. In both setups the up-scattered neutrons experienced many collisions with the walls of the storage volume before they could reach the detector. This sets the upper energy boundary for the detected neutrons and affects the detection efficiency of up-scattered neutrons.

The experiments with direct detection of up-scattered neutrons spectra may be interesting for better understanding the up-scattering mechanism.

The measured effect in the cited experiments – the number of up-scattered neutrons in storage time T is the experimental integral:

$$N_{exp} = \int_0^T \int_{E_i^{(1)}}^{E_i^{(2)}} \int_{E_f^{(1)}}^{E_f^{(2)}} \varphi(E_i, t) S \epsilon_{eff}(E_f) w(E_i \to E_f) dE_f dE_i dt \quad (1)$$

[a] e-mail: pokot@nf.jinr.ru

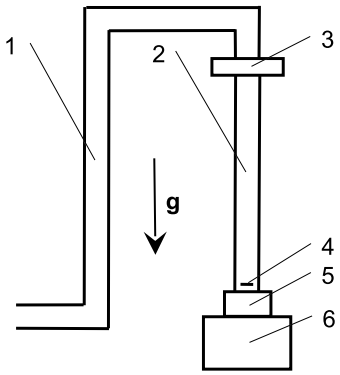

Fig. 1. Scheme of the experiment: 1 – Neutron guide, 2 – Storage tube, 3 – UCN valve, 4 – Sample, 5 – Collimator, 6 – Neutron detector.

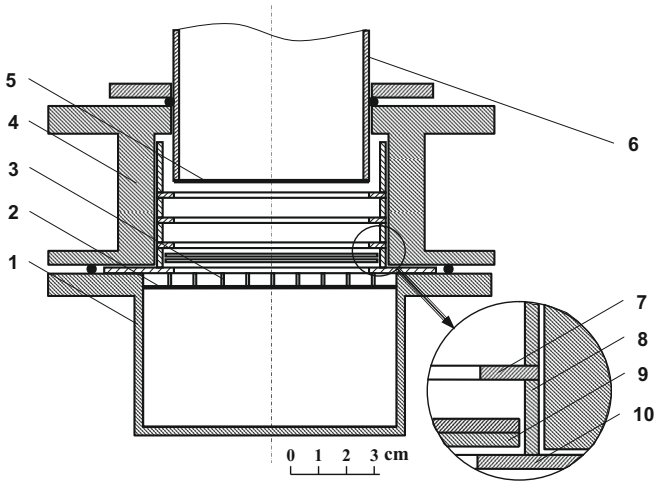

Fig. 2. Geometry of the collimator: 1 – Detector, 2 – Al 100 μm membrane, 3 – Supporting stainless steel grid, 4 – Vacuum case of the collimator, 5 – Sample foil, 6 – Stainless steel storage tube, 7 – Cadmium rings with polyethylene rings at the upper side, 8 – Cadmium rings, 9 – Si and Rh absorbers, 10 – Cadmium rings.

over the storage time and over the incident and final UCN energies E_i and E_f, $\varphi(E_i, t)$ is the time and energy dependent flux of incident stored neutrons, S is the area of the scattering sample, $\epsilon_{eff}(E_f)$ is the efficiency of detection of up-scattered neutrons including the probability to survive in the storage volume before being detected, $w(E_i \rightarrow E_f)$ is the probability of up-scattering. The incident neutron spectrum $\varphi(E_i, t)$ in these experiments was restricted by the experimental conditions: the upper boundary was $E_i^{(2)} \sim 50$–60 neV, the highest energy of the detected up-scattered neutrons $E_f^{(2)}$ was about 200 neV – the boundary energy of stainless steel wall of the storage barrel.

The total intensity of up-scattered neutrons is rather low – several neutrons per second to 4π solid angle even at the highest total up-scattering probability $\sim 10^{-4}$ for cleaned surfaces [1] and contemporary maximum UCN fluxes of the order of 10^3 cm^{-2} s^{-1}.

In the present work we describe the method of the measurement of the neutron spectral change during UCN storage in traps and report on a new measurement of the UCN up-scattering from solid surfaces. Compared to our previous work [21] we increased the number of samples and measurements to study reproducibility of results and concentrated on the method of inferring the neutron spectra from the experimental data.

In comparison with the publications [4–12]. the spectrum of incident neutrons was expanded to higher energies: 150–200 neV, e.g. up to the boundary energy of typical storage materials: copper, stainless steel; the energy of detected up-scattered neutrons was expanded as much as possible – from the UCN energy range to the thermal one.

2 Experimental method

The scheme of the experiment is shown in Figure 1. The experimental setup is not significantly different from the previous one [21]. The neutrons from the ILL UCN turbine source [22] entered through the neutron guide 1 into the vertically positioned stainless steel storage tube 2 (internal diameter 6.6 cm and length ~70 cm), which, after being filled with neutrons, was closed on the upper side with the UCN valve 3. The function of the vertical section of the neutron guide 1 was to decelerate the neutrons emerging from the UCN source.

In the previous experiment [21] we tried both vertical and horizontal positions of the storage tubes, the horizontal position was used with the Al storage tube for the measurement of up-scattering of UCN with lower energy – below ~53 neV – the Al boundary energy. In this work we used mostly vertical position.

On the detector side the tube was closed vacuum tight with the investigated sample foil 4: 8 μm copper foil (Goodfellow, 99.9% purity), or 10 μm teflon foil, or diamond like carbon (DLC) deposited on a 100 μm Al foil.

The neutron detector 6 was a gas filled ^{3}He (10 mbar) and Ar (1 atm) proportional counter separated from the sample foil by 33 mm vacuum gap.

Information on the spectrum of the neutrons propagating through the sample foil was obtained by measuring the time dependent neutron count rate for various thicknesses of neutron absorbers. These absorbers were placed inside the Cadmium collimator 5 between the detector 6 and the sample 4 irradiated by the incident neutrons in the storage volume. The construction of the Cadmium collimator (Fig. 2) provided non-reflection of neutrons, propagating through the sample foil, from the side walls of the collimator. This was achieved by placing 1 mm thick polyethylene rings at the upper sides of the collimator ribs 7. Polyethylene has low negative Fermi potential for neutrons (~–8 neV) so that neutron reflection from its surface is negligible. The neutrons propagated through or scattered from the sample and intersecting the polyethylene rings, after thermal up-scattering in polyethylene should be captured in Cd.

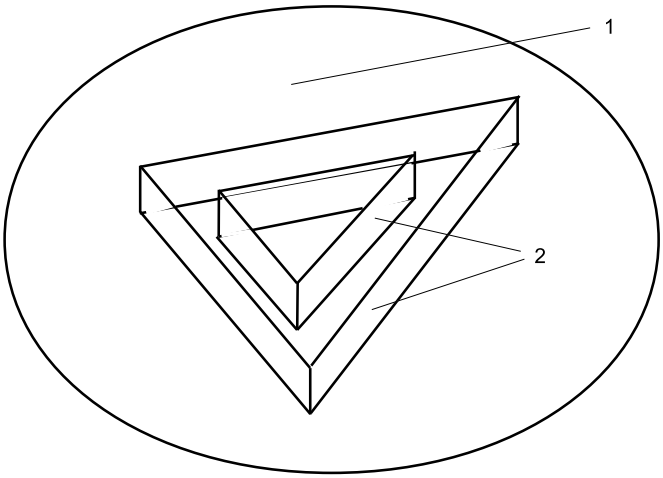

Fig. 3. Geometry of additional scatterers at the surface of the sample foil: 1 – Sample foil, 2 – Additional foil scatterers.

Two kinds of absorbers were used: Si wafers in stacks from 0.5 mm up to 28 mm, and Rh foils: from 0.1 mm up to 0.5 mm. The neutron transmission and scattering characteristics of Si wafers were investigated in special experiments with the use of the differential spectrometer of very cold neutrons [23]. It was found [21] that the neutron total cross section for Si wafers obeys the inverse velocity law in the UCN and very low energy range, with the macroscopic cross section $\Sigma = 25$ cm^{-1}/v (m/s). The inverse velocity law is valid for Rh [24] in the cold and thermal neutron energy range. It is also important that Si wafers, in contrast to practically all tested materials, did not show any angular spreading of the collimated ($\theta_{collim} = 0.07$ rad) UCN beam. It means that due to perfect crystal homogeneity of Si the neutron trajectory in Si absorber is a straight line, and the only outcome of UCN interaction with Si is neutron capture and thermal up-scattering.

In the case of copper and teflon samples in some measurements the additional scatterers from similar foils were placed at the surface of sample foil inside the storage tube. This increased the count rate of up-scattered neutrons. The additional scatterers had the form of triangular prism 2.4 cm in height with all its surface open to the UCN flux in the storage tube (Fig. 3). The measured count rate of up-scattered neutrons relative to the incident UCN flux density was found to be proportional to the total area of the scatterer, it means that the latter was the main source of the measured up-scattered neutrons.

The background count rate was measured when the UCN valve 3 was closed for a long time – for dozens of minutes or hours, so that the UCN density in the storage tube vanished and the UCN flux at the sample dropped to zero.

In contrast to the experiments of references [4–13,20] where only neutrons up-scattered back from the reflecting surface were detected, in our measurements mainly neutrons up-scattered inside and propagating through the sample foil could reach the detector.

As can be seen from the geometry of the experiment we detected the up-scattered neutrons with the energy higher than the boundary energy of the sample foils, which is 165 neV for Cu and 125 neV for teflon. The boundary energy of the DLC depends on the content of sp^3 diamond in the material which is not known precisely in our sample. The boundary energy of pure diamond with the density 3.52 g/cm^3 is 305 neV. The slow neutron reflectivity experiment [25] yielded the boundary energy of their DLC foil ∼220 neV, the data of reference [26] give the boundary energy ∼250 neV for 45% sp^3 diamond content.

As it follows from geometrical consideration (Fig. 1), the incident UCN spectrum at the level of the sample foil during storage time was restricted from below by 90 neV – gravitational acceleration of "zero" energy neutrons between the entrance to the vertical section of the neutron guide above the UCN valve 3 and the sample. The upper boundary of the stored UCN spectrum, after disappearance of super-barrier neutrons from the storage tube, was determined by the boundary energy of the sample foil: copper or teflon; in the case of DLC it is restricted by the boundary energy of the stainless steel tube 200 neV.

Time dependence of the neutron count rate was measured from the moment of opening the UCN valve (beginning of the filling the storage tube with neutrons) for 120–130 s. The filling time was 20 s. The time change of the incident UCN flux density in the storage tube was measured in special experiments when the thin sample foil, closing the storage volume, was covered from below with a 2 mm thick copper plate, non-transparent for the UCN, both had a small 2.5 mm diameter hole. The UCN loss from the storage volume through this small hole practically did not disturb the UCN density in the storage volume, the estimated UCN efflux through this hole was about two orders of magnitude lower than the losses due to neutron capture and up-scattering by the sample and the walls of the storage tube. At the same time the neutron count rate through small hole was several orders of magnitude higher than the count rate of up-scattered neutrons in this measurement. This count rate gives the time dependence of the UCN flux density at the sample. The maximum UCN flux density measured in this way: ($\int_{E_i^{(1)}}^{E_i^{(2)}} \varphi(E_i,t)dE_i$ (Eq. (1))) at the first moment after the filling was $\sim(1-2)\times 10^3$ cm^{-2} s^{-1} depending on the sample.

3 Experimental results

Figure 4 shows one typical example of the time dependent detector count rate for the measurements with a small hole and when the storage tube was closed with the sample foil. Typical UCN storage time was between ∼28 and ∼20 s, the latter figure corresponds to the measurements with additional scatterers. The measured storage time $\tau \approx \langle d\rangle/\langle\mu\rangle\langle v\rangle$, where $\langle d\rangle$ is the mean UCN free path length between collisions with the walls, $\langle v\rangle$ – the mean UCN velocity, and $\langle\mu\rangle$ is the probability of the UCN loss per one collision, corresponds to $\langle\mu\rangle \sim 5\times 10^{-4}$.

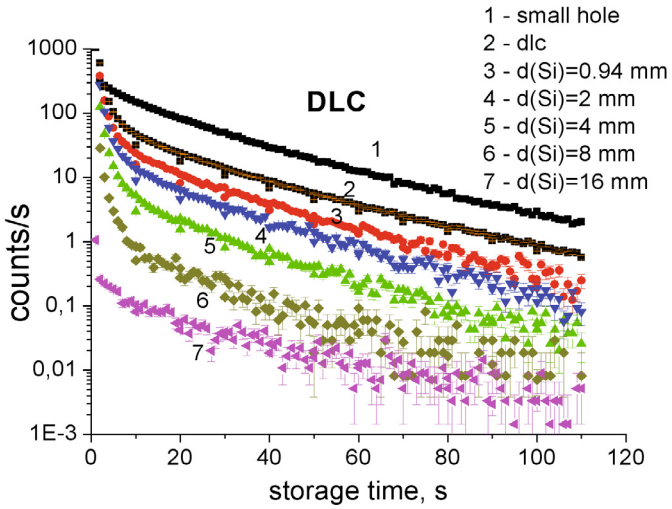

Fig. 4. (Color online) Time dependent count rate for the DLC sample foil: 1 – The UCN flux density measured through 2.5 mm diameter hole in the sample foil, 2 – The count rate through the DLC foil at the 100 μm Al substrate, no additional absorber, 3–7 – The count rate through the DLC foil with different Si absorbers between the scatterer and the neutron detector. The time shown from the moment of opening of the UCN valve after the filling time 20 s.

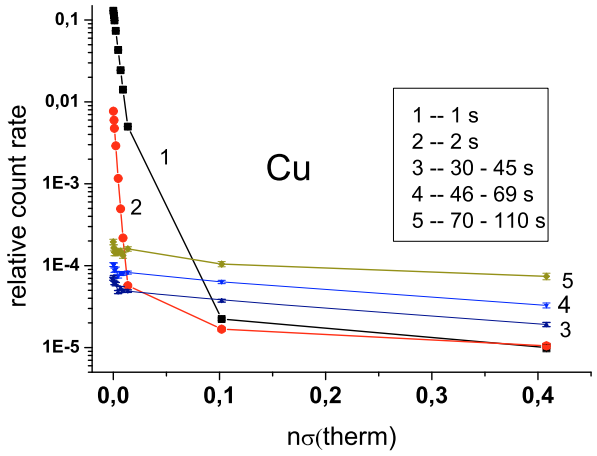

Fig. 5. (Color online) The neutron count rate (relative to the incident UCN flux) from the copper surface as a function of the absorber thickness in the $n\sigma_{therm}$ units in the full range of used absorbers. The straight lines connect the experimental points.

The time dependent neutron count rate (Fig. 4), in the measurements when the storage tube is closed with sample foil, consists of two parts. The first part shows rapid decrease of the count rate as a function of time. It represents the "cleaning" process when the super-barrier neutrons, with energy larger than the boundary energy of the storage tube or the sample, leave the storage volume propagating through the sample foil or the walls of the storage volume.

Neutrons travelling with velocity v at an angle θ with respect to the surface are absorbed in collision with the wall with boundary velocity v_b if $v \sin\theta > v_b$. Integration over solid angle of isotropically incident neutrons gives the probability of absorption $w = 1 - (v_b/v)^2$. For neutrons with the energy E close to the boundary energy $E_b w \approx (E - E_b)/E_b$. For example at $E - E_b = 1$ neV $w \sim 2\times10^{-3}$. During 30–40 s super-barrier neutrons experience several thousands collisions with the walls of the tube and the surface of the sample and are captured with probability close to unity. The measurement with the small hole does not show this rapid decline in the count rate. It means that the density of super-barrier neutrons is small relative to the total UCN density in the storage volume but their transmission probability through thin sample foil is high enough so that the "cleaning" process is well detected.

The second part of the neutron count rate corresponds to the sub-barrier UCN storage time, beginning from ~30–40 s, when only the sub-barrier neutrons are contained in the storage tube. During this time only up-scattered neutrons can pass through the sample foil to the neutron detector. The characteristic time of decline of the count rate coincides well with the characteristic time for the sub-barrier UCN storage curve measured with the small hole. These parts of the storage curves should be taken into consideration in inferring the sub-barrier UCN up-scattering probability.

Figure 5 shows the example of the count rate of neutrons through the copper sample foil relative to the incident neutron flux through a small hole as a function of the absorber thickness for different time intervals of UCN storage with the copper sample. For the unification of the data for Si and Rh absorbers with very different cross sections of neutron absorption at very low energies (the ratio $\sigma_{tot}(\mathrm{Rh})/\sigma_{tot}(\mathrm{Si}) = 618$) the absorber thickness is shown in the universal units $n\sigma$ for the neutron of 25.4 meV. It is seen that the absorption curves consist of two very different parts: steeply falling curve in the beginning and the slowly falling one when only strongly absorbing Rh foils are able to attenuate the flux of up-scattered neutrons from the sample to the neutron detector.

Thus these curves demonstrate that the spectra of up-scattered neutrons consist of two parts: very low energy neutrons with large absorption cross section and the "high energy" thermal part.

There is one feature of this curves which is still not understood: the rise of the relative count rate of thermally up-scattered neutrons as a function of time observed for copper samples. For the teflon samples this effect is absent, for the DLC is much weaker.

Possible physical reason for that may be the change of the spectra of incident neutrons: the neutrons with higher energies are lost with higher probability, and the spectrum of stored neutrons is smoothed with time. Thus the observed effect should mean that the thermal up-scattering probability is increased with decreasing energy of incident neutrons. Different models of distribution of up-scatterers at the surface and in depth of the reflecting wall were considered. The observed behavior of up-scattering could be

obtained only with very thick layer of hydrogen-containing substance at the copper surface, but in this case the up-scattering probability turns out to be abnormally large, what is not observed in the experiment.

Methodical cause of this effect could be the time-dependent decrease of the detector efficiency in the measurements of the incident flux through small hole in result of decreasing energy of the stored neutrons. This was investigated in special measurements of the incident flux through small hole. In these measurements the neutrons after propagating through the hole were gravitationally accelerated in the additional vertical neutron guide 0.5 m long. No essential change was found in comparison with the measurement without additional neutron acceleration. One more possible explanation could be the spectral change (decrease in the energy) of up-scattered neutrons with time (with decreasing energy of stored neutrons) so that the detection efficiency of up-scattered neutrons is increased. The energy resolution of our measurements of thermally up-scattered neutrons was rather low so that no clear conclusion can be made. On the other hand this effect does not change the conclusions about low energy up-scattering because for each time interval the data for thick absorbers (Rh) are subtracted.

The detection efficiency of the neutron with the velocity v, intersecting the sensitive volume of the detector after passing through the absorber, is

$$\epsilon_{eff}(v,\theta,\mathbf{r},\mathbf{r}',absorber) = e^{-d_{abs}\Sigma_{abs}(v)/\cos\theta} \times \left(1 - e^{l_{det}(\mathbf{r},\mathbf{r}')\Sigma_{det}(v)}\right), \quad (2)$$

where d_{abs} is the thickness of the absorber, θ is the angle of the neutron trajectory with respect to the absorber surface normal, $\Sigma_{abs}(v)$ is the macroscopic cross section of the absorber for the neutron velocity v, $l_{det}(\mathbf{r},\mathbf{r}')$ is the length of neutron trajectory inside the detector, depending on the coordinates $\mathbf{r}$ and $\mathbf{r}'$ of points of entry into and emergence from the detector volume, $\Sigma_{det}(v)$ is the macroscopic cross section of the neutron absorption by ^{3}He nuclei in the detector volume.

Figure 6 shows the Monte Carlo simulated neutron detection efficiency as a function of the neutron velocity and the thickness of Si absorber:

$$\epsilon^{av}_{eff}(v,absorber) = \langle \epsilon_{eff}(v,\theta,\mathbf{r},\mathbf{r}',absorber)\rangle_{trajectories}. \quad (3)$$

The efficiency is obtained as a result of averaging over all neutron trajectories in an assumption of the cosine angular distribution for the up-scattered neutrons with respect to the sample surface normal. The neutron reflection from Al window of the neutron detector has been taken into account in these simulation.

The measured count rate of the detector for the particular absorber is the result of integration:

$$N^{exper}_{absorber}(t) = \int \varphi(v,t)\epsilon^{av}_{eff}(v,absorber)dv \quad (4)$$

where $\varphi(v,t)$ is the velocity dependent neutron flux.

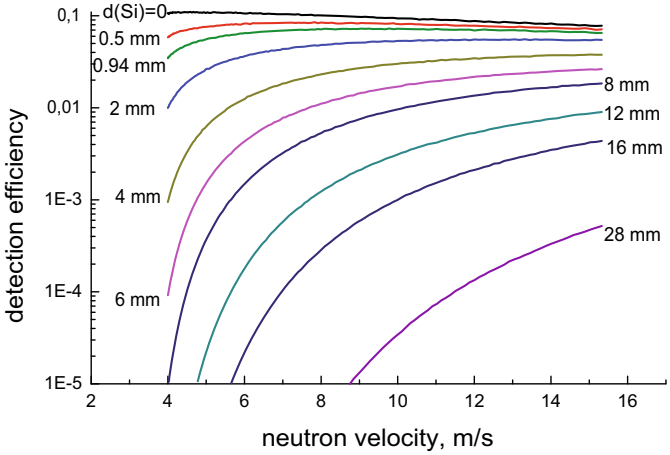

Fig. 6. (Color online) Monte Carlo simulated neutron detection efficiency in geometry of the experiment as a function of neutron velocity and the thickness of Si absorber.

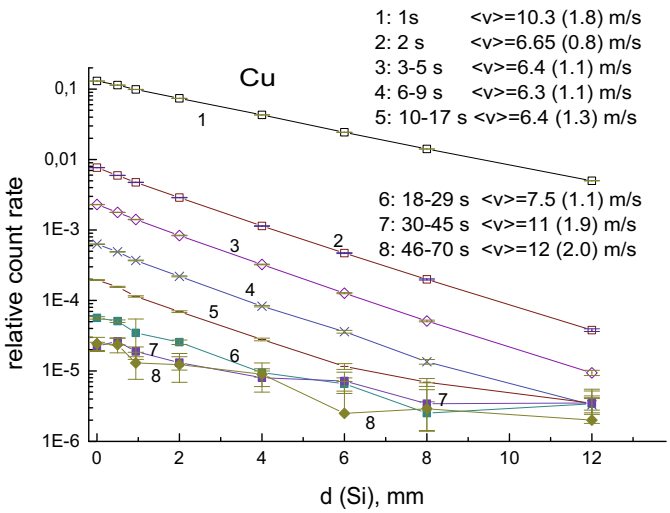

Fig. 7. (Color online) The neutron count rate (relative to the incident UCN flux) from the copper surface as a function of Si thickness after subtracting the contribution of up-scattering to the thermal energy range. The inferred neutron mean velocities and half-widths of the Gaussian distributions (in brackets) for corresponding storage time intervals are shown in the insert. The curve for the storage time intervals 71–100 s is not shown in view of overlapping with the neighboring ones. The inferred mean velocity for this interval is 12.5 m/s. The straight lines connect the experimental points.

The number of neutrons detected with the ith thickness of Si absorber during some time interval Δt of neutron storage is:

$$N_i = \int_{\Delta t}\int \varphi(v,t)\epsilon_i(v)dvdt, \quad (5)$$

where $\epsilon_i(v)$ is the neutron detection efficiency for ith Si thickness of Figure 6 and $\varphi(v,t)$ is the velocity dependent neutron flux during this time interval.

Figures 7–9 show the low energy parts of the experimental absorption curves for different time intervals of

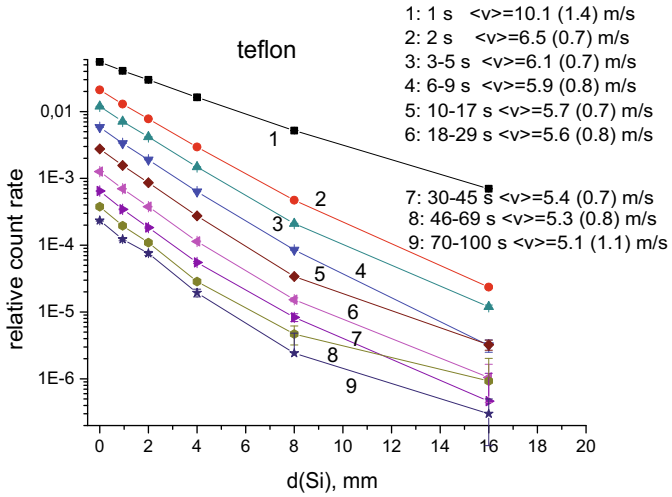

Fig. 8. (Color online) The neutron count rate (relative to the incident UCN flux) from the teflon surface as a function of Si thickness after subtracting the contribution of up-scattering to the thermal energy range. The inferred neutron mean velocities and half-widths of the Gaussian distributions (in brackets) for corresponding storage time intervals are shown in the insert. The straight lines connect the experimental points.

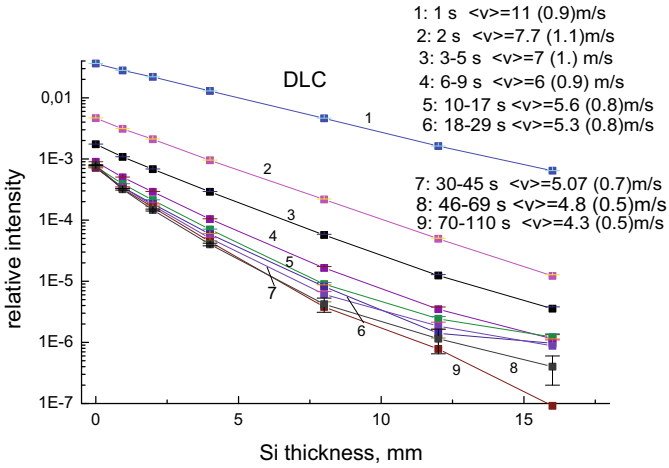

Fig. 9. (Color online) The neutron count rate (relative to the incident UCN flux) from the DLC surface as a function of Si thickness after subtracting the contribution of up-scattering to the thermal energy range. The inferred neutron mean velocities and half-widths of the Gaussian distributions (in brackets) for corresponding storage time intervals are shown in the insert. The straight lines connect the experimental points

neutron storage and three different samples. They were obtained after subtraction of extrapolated slowly falling parts, the latter being approximated by the one-exponent functions.

The time averaged spectra $\varphi(v) = \langle\varphi(v,t)\rangle_{\Delta t}$ for different time intervals Δt of UCN storage were inferred from the experimental data (Figs. 7–9) by the least squares method in different assumptions about the forms of spectra.

As is well known unfolding the true spectra belongs to a class of ill-posed problems. It is so especially in our case when the number of points is small and the detector response function has smooth shape. It is sometimes useful to fold the theoretically predicted true distribution with the estimated response matrix (the Monte Carlo simulated detector efficiency for different absorber thicknesses in our case) and compare thus folded theoretical spectrum (the count rate as a function of the absorber thickness in our case) with the measured one. But in our case the functional form of the distribution is unknown. We used the least squares method, trying to find the best solution for this functional form in the sense of minimum χ^2.

First, the simplest "monochromatic" approximation was used

$$\varphi(v) = a_1 e^{-((v-a_2)/a_3)^2}, \tag{6}$$

described by Gaussian, characterized by the amplitude in the maximum of the distribution a_1, the mean velocity of neutrons a_2, and the half-widths a_3. The inferred results for the mean velocities and half-widths are shown in the inserts in Figures 7–9 for different time intervals. In most cases χ^2 per degree of freedom is between 1 and 2 excluding several cases when it exceeds 2.

One can see the change of neutron spectra from higher velocities ~10 m/s in the first moments after filling, when the super-barrier neutron transmission through the sample foil dominates in the count rate, to lower velocities, when the higher energy super-barrier neutrons have left the storage tube. At longer storage times, greater than ~30–40 s, the neutron spectra show different behavior for different samples. In the case of teflon at longer storage times the mean velocity of up-scattered neutrons is practically constant as a function of time and is slightly higher than the boundary velocity of teflon – 4.8 m/s. But for all three investigated copper samples this velocity becomes significantly larger than the boundary velocity for copper – 5.7 m/s reaching 11–13 m/s. For the DLC sample we unexpectedly found that the characteristic neutron velocity at long storage times is significantly lower than the boundary velocity of DLC: ~4–5 m/s in comparison with $v_{bound}(DLC) \sim 6.5$–6.9 m/s. This is a clear demonstration that the DLC foils that we had at our disposal are not perfectly dense and have micro-holes.

We also tried more detailed approximations to infer the up-scattered neutron spectra by the least squares method. Different functions were tried as an approximation for the time averaged neutron spectrum $\varphi(v) = \langle\varphi(t)\rangle_{\Delta t}$ for each of the data set of equation (5):

$$\varphi(v) = a_1 e^{-va_2}(1 - e^{-va_3}), \tag{7}$$

$$\varphi(v) = a_1 e^{-((v-a_2)/a_3)^2} e^{va_4}, \tag{8}$$

$$\varphi(v) = a_1 e^{-((v-a_2)/a_3)^2} v^{a_4}, \tag{9}$$

etc. These kinds of the parameterizations were chosen from the consideration that the spectrum should have the form of a bump with the spectrum density falling at small and high values of velocities.

Figure 10 shows the inferred spectra for different time intervals of UCN storage with copper sample.

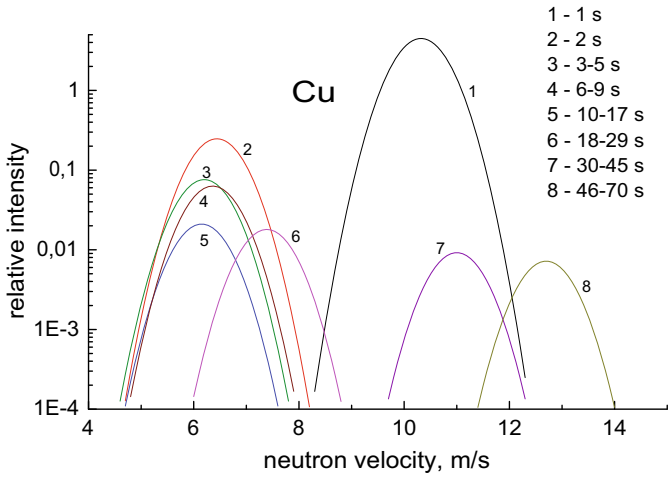

Fig. 10. (Color online) The inferred neutron spectrum for the copper sample according to equation (9). The time intervals of the UCN storage are shown in the insert.

The spectra demonstrate the same characteristics as were inferred in the monochromatic approximation (but with better χ^2): change from higher energies (super-barrier neutrons) to lower ones in the first stages of UCN storage, and then significant shift to higher energy at longer storage time.

With a larger number of points at the absorption curves (the number of used absorbers of various thickness) and better statistics it will be possible to extract more reliably the form of the inferred spectra.

The up-scattering probability with small energy transfer (obtained as a ratio of the measured flux of up-scattered neutrons to the incident UCN flux density and the sample area) was found to be equal $(2 \pm 0.2) \times 10^{-4}$ for teflon and $(5 \pm 0.9) \times 10^{-5}$ for copper samples cleaned with organic solvents.

Unfortunately for the DLC sample the very low-energy up-scattering probability could not be determined in view of overwhelming transmission of the incident UCN flux through micro-holes in the DLC layer. The probability of this transmission was found to be $\sim 10^{-3}$. Several earlier experiments [27–31] had the purpose to measure the UCN transmission through foils. The method described here may be used for obtaining information about the energy dependence of neutron transmission.

The slowly falling parts of the absorption curves were reproduced by the least squares method in monochromatic approximation for the neutron spectra. The average energy of this "high energy" part of the up-scattered neutrons was between 6 and 10 meV for different samples, the probability of "thermal" up-scattering was found to be $(5 \pm 1.8) \times 10^{-4}$ for copper sample, $(4 \pm 1.2) \times 10^{-4}$ for teflon and $(5 \pm 1.2) \times 10^{-5}$ for the DLC sample.

We also performed the measurements with the samples of Si and thin layer of Fomblin grease at the surface of Si wafer (with horizontal position of the Al storage tube, so that the energy of stored neutrons was below the boundary energy of Al – 53 neV), but the low-energy up-scattering probability turned out to be too low to infer its value and the up-scattering spectra.

In our previous experiment [32] aimed to search for the low energy UCN up-scattering from the solid (beryllium) surface the bound at a level of 10^{-5} was obtained for velocities of up-scattered neutrons higher than 15 m/s.

4 Summary

We described a method for measuring the neutron spectra during UCN storage and up-scattering from solid surfaces. The probability of up-scattering to the whole energy range higher than the boundary energy of the sample under investigation was measured for several different samples. The method consists in measuring neutron absorption curves as a function of UCN storage time. The absorbers with well-known neutron absorption cross sections: Si wafers and Rh foils were used in these measurements.

The detection efficiency as a function of neutron velocity and the thickness of absorbers was obtained in result of a Monte Carlo simulation in exact geometry of the experiment.

The time change of the spectra of stored neutrons was observed from higher mean velocities ∼10 m/s of super-barrier neutrons in the first moments after filling the storage chamber, to lower velocities, when super-barrier neutrons escape the storage tube.

The quasi-elastic and inelastic UCN up-scattering probability is determined for the samples of copper, teflon and DLC at room temperature. The spectra of quasi-elastically up-scattered neutrons are inferred in monochromatic and more detailed approximations by the least squares method.

A particular behavior of the spectra of quasi-elastically up-scattered UCN was found for different scatterers. In the case of teflon the mean energy of up-scattered neutrons was only slightly higher than the boundary velocity of teflon, but for copper this energy becomes significantly larger than the boundary energy for copper, almost reaching μeV energy range. For DLC we found significant transmission of sub-barrier UCN through the sample foil which demonstrates that the tested DLC foils are not perfectly dense and have numerous micro-holes.

The experiment was performed at the PF-2 UCN source of the Institute Laue-Langevin in the frame of the experiment 3-14-203. We are highly indebted to the staff of the ILL High Flux reactor and to Thomas Brenner for his help in the course of the experiment.

References

1. F.L. Shapiro, in *Proc. Int. Conf. Nuclear Structure with Neutrons, Budapest*, edited by J. Ero, J. Szucs (Plenum, New York, 1972), p. 259; A. Steyerl, in *Neutron Physics, Springer Tracts in Modern Physics*, Vol. 80 (Springer,

Berlin, Heidelberg, New York, 1977), p. 57; R. Golub, J.M. Pendlebury, Rep. Progr. Phys. **42**, 439 (1979); V.K. Ignatovich, *Fizika ultrakholodnykh neitronov* (Nauka, Moscow, 1986)(in Russian); V.K. Ignatovich, *The Physics of Ultracold Neutrons* (Clarendon, Oxford, 1990); R. Golub, D.J. Richardson, S. Lamoreaux, *Ultracold Neutrons* (Adam Hilger, Bristol, 1991); J.M. Pendlebury, Annu. Rev. Nucl. Part. Sci. **43**, 687 (1993)

2. *Proc. Int. Conf. Fundamental Physics with Slow Neutrons, Grenoble, 1998*, Nucl. Instrum. Meth. A **440** (2000)
3. *Proc. Int. Conf. Fundamental Physics with Slow Neutrons, Gaithersburg, USA, 2004*, J. Res. NIST **110**, (2005)
4. Y.N. Pokotilovski, Nucl. Instrum. Meth. A **554**, 356 (2005)
5. P. Geltenbort, V.V. Nesvizhevsky, D.G. Kartashov et al., JETP Lett. **70**, 170 (1999); P. Geltenbort, V.V. Nesvizhevsky, D.G. Kartashov et al., Pis'ma v ZhETF **70**, 175 (1999)
6. V.V. Nesvizhevsky, A.V. Strelkov, P. Geltenbort, P. Iaydjiev, Phys. At. Nucl. **62**, 776 (1999); V.V. Nesvizhevsky, A.V. Strelkov, P. Geltenbort, P. Iaydjiev, Jad. Fiz. **62**, 832 (1999)
7. V.V. Nesvizhevsky, A.V. Strelkov, P. Geltenbort, P. Iaydjiev, Eur. Phys. J. Appl. Phys. **6**, 151 (1999)
8. E.V. Lychagin, A.Yu. Muzychka, V.V. Nesvizhevsky et al., Phys. At. Nucl. **63**, 548 (2000); E.V. Lychagin, A.Yu. Muzychka, V.V. Nesvizhevsky et al., Jad. Fiz. **63**, 609 (2000)
9. E.V. Lychagin, A.Yu. Muzychka, V.V. Nesvizhevsky et al., Phys. Lett. B **479**, 353 (2000)
10. E.V. Lychagin, D.G. Kartashov, A.Yu. Muzychkaet al., Phys. At. Nucl. **65**, 1995 (2002); E.V. Lychagin, D.G. Kartashov, A.Yu. Muzychkaet al., Jad. Fiz. **65**, 2052 (2002)
11. V.V. Nesvizhevsky, E.V. Lychagin, A.Yu. Muzychka et al., Phys. Lett. B **479**, 953 (2000)
12. L.N. Bondarenko, P. Geltenbort, E. Korobkina et al., Phys. At. Nucl. **65**, 13 (2002); L.N. Bondarenko, P. Geltenbort, E. Korobkina et al., Jad. Fiz. **65**, 13 (2002)
13. L.N. Bondarenko, P. Geltenbort, E. Korobkina et al., JETP Lett. **68**, 691 (1998); L.N. Bondarenko, P. Geltenbort, E. Korobkina et al., Pis'ma v ZhETF **68**, 663 (1998)
14. Yu.N. Pokotilovski, Phys. Lett. A **255**, 173 (1999)
15. Yu.N. Pokotilovski, JETP **96**, 172 (2003)
16. S.K. Lamoreaux, R. Golub, Phys. Rev. C **66**, 044309 (2002)
17. Yu.N. Pokotilovski, Eur. Phys. J. B **8**, 1 (1999); Yu.N. Pokotilovski, JETP Lett. **69**, 91 (1999)
18. V.K. Ignatovich, in *Mini-Workshop "UCN Anomalies – where do we stand?", ILL, 25 November, 2000* (2000)
19. V.V. Nesvizhevsky, Phys. At. Nucl. **65**, 400 (2002)
20. A.P. Serebrov, J. Butterworth, M. Daum et al., Phys. Lett. A **309**, 218 (2003)
21. Yu.N. Pokotilovski, M.I. Novopoltsev, P. Geltenbort, Phys. Lett. A **353**, 236 (2006)
22. A. Steyerl, H. Nagel, F.-X. Schreiber et al., Phys. Lett. A **116**, 347 (1986)
23. Yu.N. Pokotilovski, M.I. Novopoltsev, P. Geltenbort, Th. Brenner, ILL Exp. Rep. 3-14-132
24. V. Mclane, C.L. Danford, P.F. Rose, *Neutron Cross Sections*, Vol.2 (Academic Press INC, 1988), p. 373; D.J. Hughes, R.B. Schwartz, *Neutron Cross Sections*, BNL-325, 2nd edn. (1958), p. 121 W. Dilg, W. Mannhart, Z. Phys. **266**, 157 (1974)
25. M.G.D. van der Grinten, J.M. Pendlebury, D. Shiers et al., Nucl. Instrum. Meth. A **423**, 421 (1999)
26. F. Atchison, B. Blau, M. Daum et al., Phys. Lett. B **692**, 24 (2006)
27. V.E. Varlamov, P. Geltenbort, V.V. Nesvizhevsky et al., Pis'ma v ZhETF **66**, 317 (1997)
28. Al.Yu. Muzychka, Yu.N. Pokotilovski, P. Geltenbort, JETP Lett. **67**, 459 (1998); Al.Yu. Muzychka, Yu.N. Pokotilovski, P. Geltenbort, Pis'ma v ZhETF **67**, 440 (1998)
29. E.V. Lychagin, A.Yu. Muzychka, V.V. Nesvizhevsky et al., JETP Lett. **71**, 447 (2000); E.V. Lychagin, A.Yu. Muzychka, V.V. Nesvizhevsky et al., Pis'ma v ZhETF **71**, 657 (2000)
30. T. Brys, M. Daum, P. Fierlinger et al., Nucl. Instrum. Meth. A **551**, 429 (2005)
31. A. Serebrov, N. Romanenko, O. Zherebtsov et al., Phys. Lett. A **335** 327 (2005)
32. Al.Yu. Muzychka, Yu.N. Pokotilovski, P. Geltenbort, JETP **88**, 79 (1999)